



Yue, T., Keller, A. G., Gosden, D. R., Bloomfield-Gadêlha, H., & Rossiter, J. M. (2023). *Hydrogel-actuated Soft Sucker with Mucus Secretion*. Paper presented at 6th IEEE-RAS International Conference on Soft Robotics (RoboSoft), Singapore, Singapore.

Peer reviewed version

[Link to publication record in Explore Bristol Research](#)  
PDF-document

## University of Bristol - Explore Bristol Research

### General rights

This document is made available in accordance with publisher policies. Please cite only the published version using the reference above. Full terms of use are available:  
<http://www.bristol.ac.uk/red/research-policy/pure/user-guides/ebr-terms/>

# Hydrogel-actuated Soft Sucker with Mucus Secretion

Tianqi Yue<sup>1</sup>, Alex Keller<sup>1</sup>, Daniel Gosden<sup>1</sup>, Hermes Bloomfield-Gadêlha<sup>1</sup> and Jonathan Rossiter<sup>1</sup>

**Abstract**—Suction is a nature-inspired adhesion strategy which has been successfully applied in industry for decades. Their high adhesive force and energy efficiency make suckers light weight and low cost. However, the requirement for compact grippers conflicts with the bulky and heavy vacuum pumps used in existing suckers. This work proposes a novel hydrogel-actuated soft sucker inspired by the octopus sucker to realise compact, compliant and adaptive suction which needs no external vacuum supply. The sucker is actuated through volume change within a double-network, thermo-sensitive hydrogel. When the hydrogel is heated, its molecular structure collapses, generating a suction force and simultaneously secreting water around the sucker rim to strengthen the suction. When the hydrogel is cooled, it reabsorbs water, recovering its initial shape and eliminating the suction force. On a dry on-land surface, the proposed sucker is capable of adhering to rough surfaces by utilizing water secretion, similar to the mucus secretion of octopus suckers. Underwater, the sucker further exhibits reversible attachment and detachment capability. Simulation results and experimental results demonstrate the practicality of this suction strategy. By applying a current of 0.3 A to generate joule heat, pressure differentials of -4.54 kPa and -4.02 kPa with respect to atmospheric pressure can be generated underwater and on land, respectively. We believe this hydrogel-actuated soft sucker is a significant new technology for next-generation safe, compliant and compact robotic suckers.

## I. INTRODUCTION

Suction is a widely-used, low-cost and energy-efficient robotic gripping strategy, widely used in industry [1]. High adhesive force, easy fabrication and high energy efficiency make suckers preferable to other adhesion methods such as electro-adhesion and gecko skins [2]–[5]. However, further development is needed to make suckers suitable for wider adoption in robotic manipulation. Firstly, to minimise the overall size and weight of the suction system, the sucker must be compact. Currently, most suckers have to be equipped with a motor-driven vacuum generator and valves [6]. In contrast, octopuses use compact sucker structures which are activated by muscles embedded in suckers. Taking inspiration from this natural organisms, robotic suckers that have an embedded actuator within the sucker would remove the

need for bulky and heavy vacuum pumps and associated components. In addition, compliance in the natural sucker helps to reduce contact impedance and surface topology mismatches between the sucker and the object. Although most state-of-the-art suckers have a thin, flexible cup surface, some rigid components [6], [7] still add rigidity and this reduces the strength of the sucker-object interface.

These two problems – removing external vacuum systems and enhancing sucker compliance – can both be solved by embedding soft actuators into the sucker. Existing work has demonstrated how actuators such as tendons [5], electro-adhesion (EA) [8], and hydrogel actuators [9], [10]. DEA-based suckers provide fast response, but the high voltage and relatively weak suction pressures generated limit their potential applications [4]. Electro-adhesion differs from deformation-induced suction by directly generating adhesive force at the surface interface. However, the adhesion strength of electro-adhesion is much less than the suction strength, which means it can only be a supplementary part of the total adhesion [8]. Previously hydrogel-based suckers are predominantly designed in the form of simple multiple-sucker films [9], [10], achieving adhesion on rough surfaces through miniature suckers. Within the field of hydrogel-based suckers, the large-scale (i.e., on the scale of octopus suckers) hydrogel sucker still remains unexplored and unexploited. In this paper, we present a novel hydrogel-actuated soft sucker which utilizes a similar suction mechanism to octopus suckers, as shown in Fig.1. Thermoelectrically induced shrinkage of the hydrogel, akin to muscular contraction within the octopus sucker, generates negative pressure for suction. When adhering to rough and dry surfaces on land, the sucker secretes water to wet the interface, enhancing suction strength and allowing an object to be picked up. When gripping an object underwater, the suction is reversible and the sucker can grip and release objects.

Actuation of the sucker is achieved by controlling the temperature of a double-network, thermo-sensitive hydrogel. A low current (0.3 A) applied to a nichrome heater coil embedded in the sucker which generates sufficient joule heat to raise the temperature of the hydrogel above its actuation temperature. The hydrogel then contracts, simultaneously generating suction and secreting water to enhance the sucker-object seal. This is a morphological analogue of the octopuses' simultaneous musculature contraction and mucus secretion during suction. In section II, we present the structure of the sucker and introduce process for optimizing the sucker design and performance using simulation. The fabrication is also presented in detail. In section III, experimental results including suction characterization and on-land

<sup>1</sup>Tianqi Yue, Alex Keller, Daniel Gosden, Hermes Bloomfield-Gadêlha and Jonathan Rossiter are with the Department of Engineering Mathematics and Bristol Robotics Laboratory at the University of Bristol, Bristol, BS8 1TW, UK {tianqi.yue, alex.keller, daniel.gosden, hermes.gadelha, jonathan.rossiter}@bristol.ac.uk

TY was funded by Chinese Scholarship Council through award 201906120027. DG is supported by is supported by the EPSRC Centre for Doctoral Training in Future Autonomous and Robotic Systems (FARSCOPE, grant EP/L015293/1). JR was supported through EPSRC research grants EP/V062158/1, EP/T020792/1, EP/V026518/1, EP/S026096/1 and EP/R02961X/1, and by the Royal Academy of Engineering as a Chair in Emerging Technologies.

Data available at: 10.5523/bris.2hzqjunnry1952q4acb9yf1va5

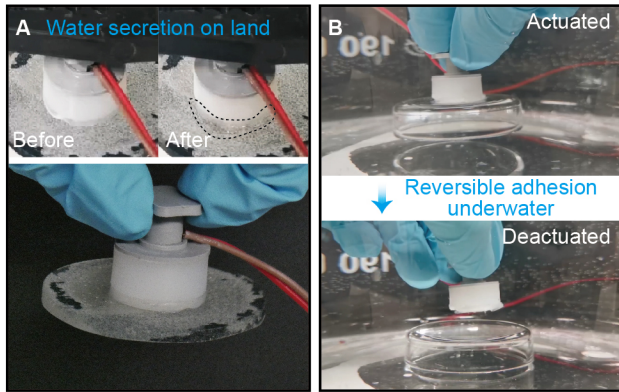


Fig. 1. Two gripping situations show the application of the proposed hydrogel-actuated soft sucker. (A) The sucker secretes water (indicated by the dashed line) to grip a dry and rough object on land. (B) The reversible adhesion can be achieved underwater.

and underwater gripping tests are presented. In section IV, we conclude this work and suggest future work.

## II. STRUCTURE, SIMULATION AND FABRICATION

The structure of the proposed hydrogel-actuated sucker is shown in Fig.2. Beneath a lid, a hollow cylindrical silicone ring surrounds the hydrogel. The inner hydrogel structure is composed of a cylindrical core and a thin circular cup extending to the rim. A heating coil is embedded in the hydrogel to generate joule heat. By joule heating, the temperature, and hence volume, of the hydrogel can be controlled. Changes in the hydrogel volume generate a pressure differential, thereby generating suction. When heating is stopped, heat transfer with the environment cool the hydrogel, allowing it to recover to its original shape by swelling, eliminating suction. A thin hydrophilic silicone pad is attached to the bottom of the hydrogel and makes direct contact with the substrate. The center of the hydrophilic silicone pad is thicker than its edge. This serves to dissipate any suction that remains after the hydrogel de-activates and reswells. During actuation, a thin layer of water is secreted from the hydrogel, aiding suction.

The octopus sucker utilizes musculature bundles to generate suction force [11], which also inspires the development of artificial suckers [12]. As Fig.3A shows, muscle contraction expands the inner volume of the infundibulum cavity to generate a negative pressure relative to atmospheric pressure, and thus suction is generated. Moreover, a mucus gland locating at the sucker rim secretes mucus to enhance suction. [13]. The enhancement of suction comes from the high relative viscosity of mucus compared to air, which reduces the leakage rate significantly on rough surfaces [14]. Similar functionality is achieved by the hydrogel-based sucker shown in Fig.3B. The thermo-sensitive network in the hydrogel is crosslinked poly(N-isopropylacrylamide) (PNIPAm), while a second interpenetrating network, crosslinked alginate, provides mechanical strength. The PNIPAm network has a transition temperature  $T_{trans} \approx 31.5$  °C. When the gel is below  $T_{trans}$ , the PNIPAm network maintains its as-fabricated

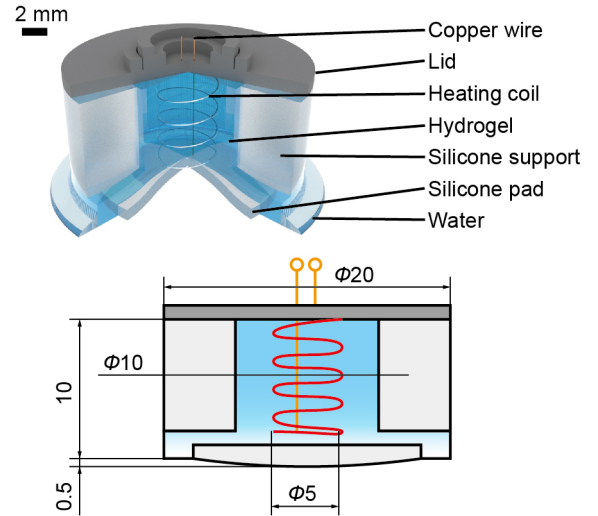


Fig. 2. Structure of the hydrogel-actuated soft sucker. Top: rendered perspective view. Bottom: half-section view with key dimensions. Unit: mm.

shape, provided it does not dry out. When the temperature of the gel exceeds  $T_{trans}$ , the PNIPAm network changes state from hydrophilic to hydrophobic. This causes the hydrogel molecular structure to collapse and release water, with consequential volume shrinkage. The transition is shown in Fig.4A. By controlling electrical current in the heating coil, the desired temperature can be obtained and the deformation of the hydrogel can be controlled. This volume change causes a negative pressure with respect to atmospheric pressure, analogous to the contraction of the octopus' sucker musculatures. Water secretion, in the meantime, is caused by the thermal collapse of the hydrogel. Since the gel is enclosed by waterproof materials, only the lower rim provides a free path for water to flow out. The hydrophilic silicone pad makes secreted water spread easily around the rim and the bottom of the sucker. This water seal works as the mucus of the octopus sucker, allowing the sucker to maintain suction for longer when working on an on-land, dry and rough surface. When the sucker is underwater, the hydrogel reabsorbs water during cooling. The suction force will be eliminated when the hydrogel recovers to its initial shape.

The thermo-actuation property of the hydrogel is characterized as shown in Fig.4B. A thin circular hydrogel sample is fabricated, then soaked in a water bath on a hotplate. By controlling the water bath temperature, the diameter shrinkage with respect to temperature change is calculated by  $\alpha = d_T/d_{20^\circ\text{C}}$ . Here  $\alpha$  is the diameter shrinkage ratio, and  $d_T$ , measured by image processing, is the diameter at temperature  $T$ . Significant diameter shrinkage occurs at  $T \approx 31.5$  °C, then stabilizes to  $\alpha = 0.66$  when  $T \geq 70$  °C. This relation will be used in the following simulations. The actuation speed should also be considered. That is, the effect of the temperature of the heating source on the hydrogel shrinking speed. The same circular hydrogel sample is moved from a room-temperature water bath (20 °C) to the hot water bath (heating source). As Fig.4C shows, the hotter the heating

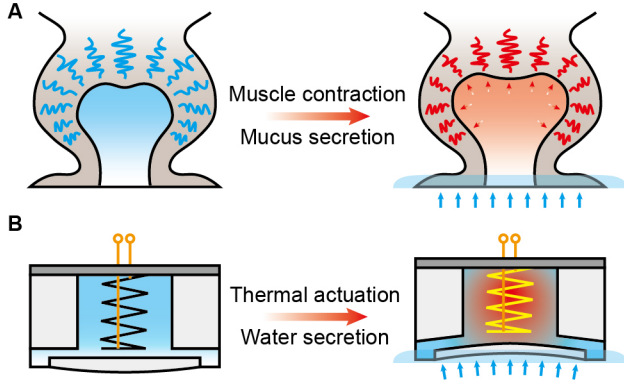


Fig. 3. Morphological analogue between the hydrogel-actuated sucker and an octopus sucker. (A) The octopus sucker contracts its musculature (illustrated by the color change from blue to red) to expand the infundibulum, generating negative pressure (relative to atmosphere). Mucus glands located around the octopus sucker rim secrete mucus to enhance the suction. (B) The proposed sucker uses electrical current to heat the hydrogel, generating suction force and simultaneously secreting water around the sucker rim.

source, the faster the shrinkage. This indicates that higher current will actuate the hydrogel faster, as a supplementary information for the following simulations.

To determine an appropriate current to actuate the hydrogel, a finite element (FE) simulation was implemented in COMSOL. The simulation model is assembled from three components: the silicone support, the hydrogel, and the hydrophilic silicone pad. The volume change of the hydrogel follows the experimental results shown in Fig.4B, expressed by a three stage function fit defined over temperature  $T$ ,

$$\alpha = \begin{cases} 1, & T < 31.5 \\ 750e^{-0.25T} + 0.7e^{-7.4 \times 10^{-4}T}, & 31.5 \leq T \leq 70 \\ 0.66. & 70 < T \end{cases}$$

We regard the volume change of hydrogel as a homogeneous transition process, which means that the temperature-controlled strain  $\alpha$  is the same along the  $x$ ,  $y$  and  $z$  axes. Using an equilibrium (static) study as the simplest case, and taking the current  $I$  applied to the heating resistor coil as the source variable, the shape deformation of the sucker is derived as the dependent variable. The environment is set as room-temperature air so the heat transfer between the sucker and environment is predominantly via fluid convection. The underwater case has faster heat energy loss than in air, but this does not significantly affect the temperature of the hydrogel core. As shown in Fig.4D, the center displacement  $d_c$  is obtained from the simulation results. This displacement is measured as the difference in position of the sucker bottom center between the undeformed state and the stationary deformed state (Fig.4E). From Fig.4D we see that the sucker shape deformation begins from 0.08 A, indicating that  $I \leq 0.08$  A cannot generate sufficient joule heat to raise the hydrogel above 31.5 °C. The center displacement significantly increases when  $0.08A < I \leq 0.12$  A. Above  $I = 0.12$  A, the center displacement does not increase

further, indicating that the sucker deformation saturates. However,  $I = 0.12$  A may not be the optimum current for actuating the hydrogel, since the actuation speed should also be taken into consideration. The simulation study generates solutions at static equilibrium and the time to achieve the stable state is unknown. Nevertheless,  $I \geq 0.12$  A will be considered the appropriate current range for subsequent experiments. The simulation results also indicate that the maximum center displacement is approximately 3.74 mm. The depth of the convex dome (0.5 mm) of the hydrophilic silicone pad (shown in Fig.2, half-section view) is much smaller than the maximum center displacement (3.74 mm), and therefore will not affect the suction. Once the current applied in the coil is turned off, the sucker will recover its original shape as the hydrogel cools and reabsorbs water. The convex hydrophilic silicone pad ensures that, when the sucker is fully deactivated, all suction will be lost and the contacted object or surface will be released.

The fabrication process of the sucker is as follows. First, the molds and the top lid are 3D printed from ABS. All the 3D printed parts are smoothed by acetone then washed in deionised (DI) water. Second, the heating resistor coil is prepared. Nichrome wire (diameter 0.1 mm, resistance 138.8  $\Omega/m$ , Sourcing Map) is wound to a helix shape with diameter of 5 mm and pitch of 2 mm. The total coil height is 8 mm. Each end of the coil is soldered to 0.1 mm copper wire. The coil is then fixed to the mold by adhesive tape.

Third, the hydrogel muscle is fabricated through a procedure modified from [15]. 200 mg alginic acid sodium salt from brown algae (alginate, Sigma) is added to 10 g DI water and mixed by centrifugal mixer (Thinky ARE-250) at 2000 rpm until clear. To this, 1 g N-Isopropylacrylamide (NIPAM, Sigma) is added and again mixed until clear. Next, 10 mg N,N'-Methylenebisacrylamide crosslinker powder (MBAm, Sigma) is added into the solution and mixed until clear. Once homogeneous, the solution is placed in a fridge (4 °C) for at least 10 minutes to reduce the rate of polymerization in preparation for the following steps. Next, 100 mg ammonium persulfate thermal initiator (APS, from Sigma) is added to the solution and mixed to clear. Because N-Isopropylacrylamide switches to a hydrophobic state above its transition temperature (31.5 °C), polymerization must be carried out at low temperatures to avoid a phase separation between the alginate and PNIPAM networks. To avoid long polymerization times, a polymerization accelerator (catalyzer) N,N,N',N'-Tetramethylethylenediamine (TEMED, Sigma) was used. After the solution is thoroughly mixed, a solution of 3  $\mu\text{L}$  TEMED dispersed in 297  $\mu\text{L}$  DI water is added into the solution. After mixing, the solution was carefully cast into the molds. The molds are left at room temperature for at least 2 hours to fully cure the PNIPAM network. The molds containing the cured gel are then soaked in calcium chloride solution (1 mol) for at least 1 hour to crosslink the alginate network. Next, the hydrogel is removed from the mold, then soaked in the calcium chloride solution for one more hour to cure the alginate network thoroughly. Finally, the gel is soaked in DI water to reswell to its initial shape.

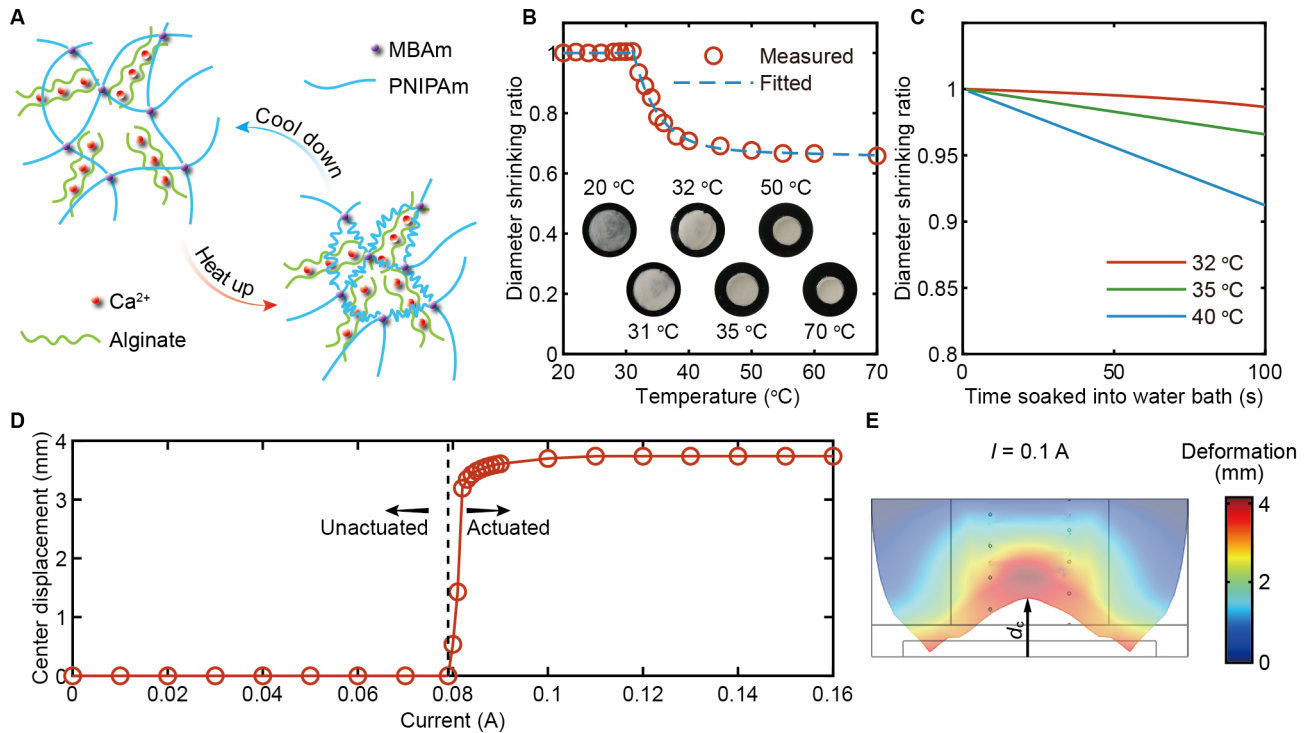


Fig. 4. Characterization of the hydrogel and simulation results. (A) The working principle of the double-network thermo-sensitive hydrogel. When heated above the transition temperature ( $T_{\text{trans}} \approx 31.5$  °C), the PNIPAm network collapses, causing volume shrinkage and water release. After cooling, the PNIPAm network expands back to its initial shape by absorbing water. (B) Measured diameter shrinking ratio of the hydrogel with temperature increase. A rapid volume shrinkage occurs at 31.5 °C, then decreases to  $\alpha \approx 0.66$  when  $T > 70$  °C. (C) Shrinkage ratio with respect to time for different water bath temperatures, indicating the temperature of heat source influences actuation speed. (D) Results of FE analysis of configuration in (E), showing equilibrium position of centre of the hydrogel for different applied electrical currents. A current less than 0.08 A does not cause hydrogel deformation since induced temperature is lower than  $T_{\text{trans}}$ . Above 0.12 A, the sucker displacement reaches its maximum of 3.74 mm, suggesting a current of at least 0.12 A will lead to largest suction force. (E) Simulated deformation of FE model when  $I = 0.1$  A. Center displacement  $d_c$  is measured from the undeformed bottom center to the deformed bottom center. The black frame is the undeformed shape of the sucker.

Fourth, the silicone support and the hydrophilic silicone pad are fabricated. For the silicone support, 4 g Dragon Skin 10 NV part A (Smooth-On) and 4 g part B is stirred thoroughly. The liquid silicone is then moved to a vacuum chamber to remove bubbles. The liquid silicone is cast into the molds then moved into the oven (40 °C) for 1 hour to cure. For the hydrophilic silicone pad [16], 2 g Ecoflex 00-30 part A (from Smooth-On) and 2 g part B are weighed and mixed. 60 mg poly(dimethylsiloxane-b-ethylene oxide) (PBP, Polysciences) is added into the liquid silicone, stirred thoroughly, degassed, cast into the molds, and moved into the oven (40 °C) for 4 hours to cure. Finally, a thin layer of super glue (Loctite) is brushed onto the surface for bonding the hydrogel and silicone components.

### III. RESULTS

Simulation results are derived by the stationary FE study. We evaluate the actuation speed of the gel by observing the hydrogel color change. The shrinkage of the proposed hydrogel causes a color change from transparent to white, which is a sufficient indicator to show that the hydrogel has actuated. To clearly demonstrate the color change, a hydrogel sample was prepared as shown in the Fig.5 inserts. Different currents  $I = [0.1, 0.2, 0.3]$  A are applied to heat up the

hydrogel for 2 minutes. The color change from transparent to white is evaluated by image processing in MATLAB. Fig.5 shows the normalised grayscale intensity of the hydrogel region. Although simulation results indicate that a current of 0.1 A can actuate the hydrogel, no actuation of the test sample was measured within two minutes. We consider two possible causes for this variation. First, the experimental condition has a larger surface area exposed to air, which causes faster heat dissipation than in the simulation. Second, the simulation generates a stationary result, and a long time may be required before equilibrium is reached. The results shown in Fig.5 only record the first 120 seconds after the current is applied, which may not be long enough to reach equilibrium. However, the experiment is still sufficient to determine how large a current should be applied. When  $I = 0.3$  A, the normalized actuation intensity at  $t = 120$  s is large ( $\sim 1.16$ ), as indicated by the much whiter color of the top insert of Fig.5.  $I = 0.4$  A was also tested, but bubbles were observed during actuation. Therefore, in the following results we use  $I = 0.3$  A to actuate the sucker.

Characterization of the suction pressure differential was then conducted. A tank filled with water at room temperature provides an underwater test environment. The bottom surface



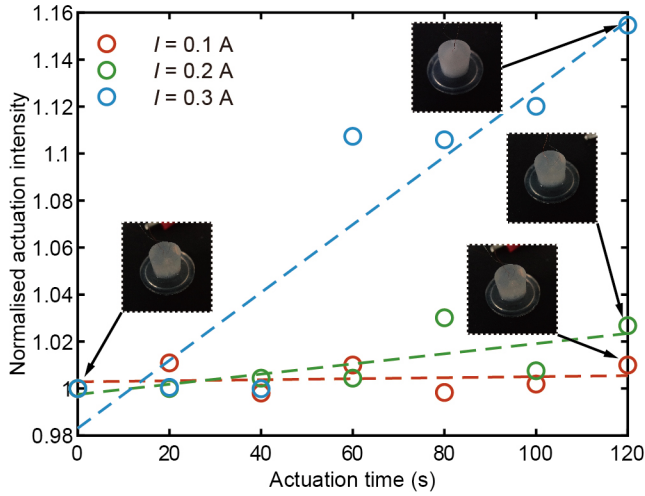


Fig. 5. The normalised actuation intensity over actuation time. Inserts: photo of hydrogel at different times. A linear fit to experimental data reveals the mean actuation speed (slope of dashed lines).  $I = 0.1$  A actuates the hydrogel very slowly, and no obvious slope can be seen.  $I = 0.3$  A actuates the hydrogel fastest, without damaging the hydrogel.

of the tank is made from a PMMA sheet. A small hole at the bottom of the tank connects to a pressure sensor (SSCDRRV015PDAA5, Honeywell) through a thin tube to monitor the pressure change. Switching of the current is manually controlled. When the power is turned on, 0.3 A current is applied through the heating resistor coil. when the power is turned off, the sucker loses heat to the environment and cools. To implement on-land (i.e., not underwater) suction experiments, water is removed from the tank.

Characterization results are shown in Fig.6. Fig.6A and Fig. 6B show the actuation and de-actuation of the thermo-actuated hydrogel sucker in the underwater case and the on-land case respectively. From 0 s to the moment indicated by the black dashed line ( $\sim 300$  s), the sucker was actuated with a current of 0.3 A. At this time the current supply was turned off. At the beginning of the actuation cycle, the pressure differential  $\Delta P = 0$  kPa for a short period for both cases. This corresponds to the initial center displacement  $d_c < 0.5$  mm which is needed to retract the convex centre of the sucker, after which suction can be established. At 74 s and 94 s for the underwater case and on-land case respectively, the suction region has formed and the pressure differential starts to increase. Approximately 300 seconds after the actuation, the suction pressure differential reaches the maximum in both cases, meaning the sucker is at thermal equilibrium with the environment and the hydrogel has reaches its maximum shrinkage. The maximum pressure differentials achieved by the underwater case and the on-land case were -4.54 kPa and -4.02 kPa respectively. We suggest that this difference is caused by the water-seal enhancement of the suction which is a little more effective under water [17]. When de-actuation begins (dashed lines), the pressure drops rapidly then slowly converges to the fully de-activated state. For the underwater case, after approximately 11500 seconds ( $\sim 3$  hours, 12 minutes) the suction pressure differential resets to zero.

This process is caused by the hydrogel reabsorbing water after cooling down. During reswelling, the bottom center of the sucker extends, and finally eliminates all suction. However, for the on-land case, the sucker cannot quickly eliminate the suction force (as shown in Fig.6B). This is because the water secreted during the actuation period cannot be completely reabsorbed due to evaporation and substrate wetting. Therefore, even though the hydrogel has been cooled down below the transition temperature, there is not enough water for the hydrogel to regain its original shape. In this case, the sucker does not exhibit fully reversible suction, and a suction of approximately 1.9 kPa remains. However, this smaller suction can be broken by hand, or will leak away over a longer period time. The simultaneous water secretion during suction on-land enables it to pick up rough objects, and it can be fully reset by soaking it in water.

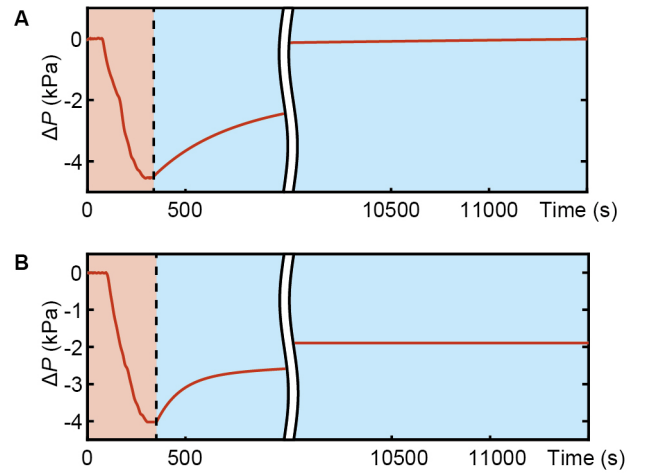


Fig. 6. Suction performance characterization of the hydrogel-actuated sucker. (A) Underwater case. (B) On-land case. Red regions: actuation period (0.3 A current on). Blue region: de-actuation period (current off). The sucker reswells faster and shows reversible suction underwater, but does not fully de-activate on-land.

Next, the water secretion performance of the hydrogel-actuated sucker is evaluated by the following on-land roughness tests. Several flat samples with different roughness are fabricated by replicate molding of rough silicon carbide particulate surfaces of 360 (smoothest), 220, 180, 120, 80, and 60 (roughest) grit using clear epoxy (JDiction).

Before the roughness experiments, the sucker was fully swelled in water. The rough epoxy resin sample was placed on an acrylic sheet. A camera recorded the color change from underneath. The sucker was then placed on the rough sample and was held in place with a clamp to provide a light downward squeezing force. Approximately 3 minutes after actuation, a clearly visible water rim is seen around the sucker (can be seen in Fig.1A). When the clamp is removed, the sucker can pick up the rough sample and maintain the grip. All the rough samples were tested three times. If the sucker successfully picks the sample up and maintains suction for 30 seconds, this grip is recorded as a successful grip. All three grips on 360, 220, 180 and

120 grit samples were successful, while the sucker fails to generate suction on 80 and 60 grit samples. This means the sucker can undertake industrial tasks involving suction onto objects with dry surfaces that are not rougher than 120 grit. Demonstrations of picking up samples are given in Supplementary Video S1.

Finally, an underwater suction test of the hydrogel sucker was undertaken. A glass dish is placed on the bottom of a tank. The tank is filled with room-temperature water. As with the on-land test, the sucker is gently pushed onto the glassware then actuated for 3 minutes. The established suction is then demonstrated by picking the dish up from the tank bottom (see Fig.7A). The current is then turned off to de-actuate the sucker. After de-actuation for 3 hours, the suction force is fully eliminated and the sucker detaches from the glass surface (see Fig. 7B, Video S2). After too much actuation, however, the hydrogel became brittle due to the applied stress during the experiments.

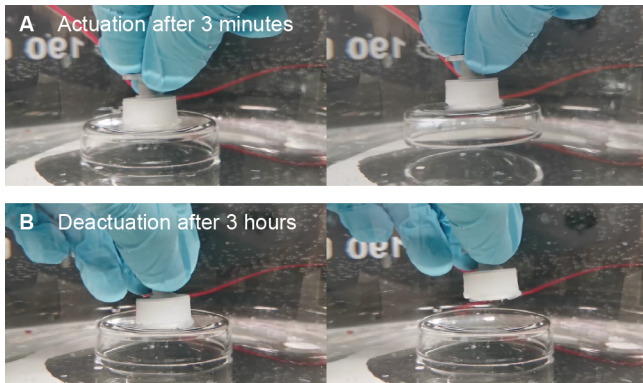


Fig. 7. Underwater reversible suction of the sucker. (A) Suction force is generated by actuating the sucker (applying 0.3 A current) for 3 minutes. A glass dish is picked up by the sucker. (B) Suction force is eliminated by de-actuating the sucker.

#### IV. CONCLUSION

In this paper, we have demonstrated a novel hydrogel-actuated soft sucker with an octopus-like suction mechanism. Two aspects make the sucker morphologically analogous to octopus sucker: the hydrogel deformation mimics muscle movement, and the water secretion mimics the mucus secretion of the octopus sucker. This sucker can be used to grip dry and rough objects on land, or reversibly grip and release objects underwater.

By applying an actuation current of 0.3 A for 300 seconds at most, the sucker achieves maximum suction pressure differentials (relative to atmospheric pressure) of -4.54 kPa underwater and -4.02 kPa on land. By autonomous actuation-driven expression of water into the sucker-substrate interface, the suction on rough surfaces is improved. Because of this, the proposed hydrogel sucker is capable of picking up samples as rough as 120 grit. For underwater application, the hydrogel embedded in the sucker reabsorbs water from the environment when the current is turned off, which enables the sucker to reversibly generate suction.

The relatively long activation-deactivation time might preclude the sucker from some practical applications, but can be addressed by future improvement. For example, using hydrogel sponge which provides a larger exposed surface area of the hydrogel can increase the activation-deactivation speed. In conclusion, we believe this hydrogel-actuated sucker provides a new path for achieving compact and soft suction for next-generation robotics.

#### REFERENCES

- [1] Piab, "Modular suction cups," <https://www.piab.com/suction-cups-and-soft-grippers/modular-suction-cups/> Accessed October 19, 2022.
- [2] J. Shintake, V. Cacucciolo, D. Floreano, and H. Shea, "Soft robotic grippers," *Advanced Materials*, vol. 30, no. 29, p. 1707035, 2018.
- [3] H. Bing-Shan, W. Li-Wen, F. Zhuang, and Z. Yan-zheng, "Bio-inspired miniature suction cups actuated by shape memory alloy," *International Journal of Advanced Robotic Systems*, vol. 6, no. 3, p. 29, 2009.
- [4] N. Sholl, A. Moss, W. M. Kier, and K. Mohseni, "A soft end effector inspired by cephalopod suckers and augmented by a dielectric elastomer actuator," *Soft robotics*, vol. 6, no. 3, pp. 356–367, 2019.
- [5] S. Wang, L. Li, W. Sun, D. Wainwright, H. Wang, W. Zhao, B. Chen, Y. Chen, and L. Wen, "Detachment of the remora suckerfish disc: kinematics and a bio-inspired robotic model," *Bioinspiration & Biomimetics*, vol. 15, no. 5, p. 056018, 2020.
- [6] T. Tomokazu, S. Kikuchi, M. Suzuki, and S. Aoyagi, "Vacuum gripper imitated octopus sucker-effect of liquid membrane for absorption," in *2015 IEEE/RSJ International Conference on Intelligent Robots and Systems (IROS)*. IEEE, 2015, pp. 2929–2936.
- [7] T. Yue, W. Si, A. J. Partridge, C. Yang, A. T. Conn, H. Bloomfield-Gadêlha, and J. Rossiter, "A contact-triggered adaptive soft suction cup," *IEEE Robotics and Automation Letters*, vol. 7, no. 2, pp. 3600–3607, 2022.
- [8] Y. Okuno, H. Shigemune, Y. Kuwajima, and S. Maeda, "Stretchable suction cup with electroadhesion," *Advanced Materials Technologies*, vol. 4, no. 1, p. 1800304, 2019.
- [9] H. Lee, D.-S. Um, Y. Lee, S. Lim, H.-j. Kim, and H. Ko, "Octopus-inspired smart adhesive pads for transfer printing of semiconducting nanomembranes," *Advanced Materials*, vol. 28, no. 34, pp. 7457–7465, 2016.
- [10] D. W. Kim, K.-I. Song, D. Seong, Y. S. Lee, S. Baik, J. H. Song, H. J. Lee, D. Son, and C. Pang, "Electrostatic-mechanical synergistic in situ multiscale tissue adhesion for sustainable residue-free bioelectronics interfaces," *Advanced Materials*, vol. 34, no. 5, p. 2105338, 2022.
- [11] W. M. Kier and A. M. Smith, "The structure and adhesive mechanism of octopus suckers," *Integrative and Comparative Biology*, vol. 42, no. 6, pp. 1146–1153, 2002.
- [12] F. Tramacere, L. Beccai, F. Mattioli, E. Sinibaldi, and B. Mazzolai, "Artificial adhesion mechanisms inspired by octopus suckers," in *2012 IEEE International Conference on Robotics and Automation*. IEEE, 2012, pp. 3846–3851.
- [13] G. Accogli, G. Scillitani, D. Mentino, and S. Desantis, "Characterization of the skin mucus in the common octopus *Octopus vulgaris* (Cuvier) reared paralarvae," *European Journal of Histochemistry: EJH*, vol. 61, no. 3, 2017.
- [14] A. Tiwari and B. Persson, "Physics of suction cups," *Soft matter*, vol. 15, no. 46, pp. 9482–9499, 2019.
- [15] H. Warren, M. in het Panhuis, G. M. Spinks, and D. L. Officer, "Thermal actuation of hydrogels from pnipam, alginate, and carbon nanofibres," *Journal of Polymer Science Part B: Polymer Physics*, vol. 56, no. 1, pp. 46–52, 2018.
- [16] M. Yao and J. Fang, "Hydrophilic pEO-pdms for microfluidic applications," *Journal of Micromechanics and Microengineering*, vol. 22, no. 2, p. 025012, 2012.
- [17] Y. Wang, Z. Li, M. Elhebeary, R. Hensel, E. Arzt, and M. T. A. Saif, "Water as a "glue": Elasticity-enhanced wet attachment of biomimetic microcup structures," *Science advances*, vol. 8, no. 12, p. eabm9341, 2022.